Published in final edited form as:
Neuron. 2008 May 22; 58(4): 499–506.

Direction selectivity in the retina is established independent of visual experience and early cholinergic retinal waves

Justin Elstrott[1], **Anastasia Anishchenko**[1], **Martin Greschner**[2], **Alexander Sher**[3], **Alan M. Litke**[3], **E.J. Chichilnisky**[2,*], and **Marla B. Feller**[4,*]

1*Neurobiology Section, Division of Biological Sciences, UCSD, La Jolla, CA, USA.*

2*Salk Institute, La Jolla, CA, USA.*

3*Santa Cruz Institute for Particle Physics, UCSC, Santa Cruz, CA, USA*

4*UC Berkeley, Berkeley, CA, USA*

Abstract

Direction-selectivity in the retina requires the asymmetric wiring of inhibitory inputs onto four subtypes of On-Off direction selective ganglion cells (DSGCs), each preferring motion in one of four cardinal directions. The primary model for the development of direction selectivity is that patterned activity plays an instructive role. Here we use a unique, large scale multielectrode array to demonstrate that DSGCs are present at eye-opening, in mice that have been reared in darkness, and in mice that lack cholinergic retinal waves. These data suggest that direction selectivity in the retina is established largely independent of patterned activity, and is therefore likely to emerge as a result of complex molecular interactions.

Direction selective circuity in the retina extracts motion information from the visual field and initiates reflexive eye movements, stabilizing the visual image on the retina when the animal is in motion (Faulstich et al., 2004; Stahl, 2004). Direction selective ganglion cells (DSGCs), first characterized in the rabbit retina over 40 years ago (Barlow and Hill, 1963), fall into two populations. On DSGCs project to the accesory optic system (Simpson, 1984) and mediate the slow component of the optokinetic reflex (OKR) (Oyster et al., 1972). On-Off DSGCs project to the thalamus (Stewart et al., 1971) and superior colliculus (Vaney et al., 1981) and are thought to mediate the fast component of the OKR (Oyster et al., 1972). DSGCs show robust firing to stimuli moving in the preferred, but not the null, direction of their receptive fields. On-Off DSGCs, which have been studied most extensively, form four subtypes, each preferring motion in one of the cardinal directions: nasal, temporal, dorsal, or ventral (Oyster and Barlow, 1967). Each subtype of On-Off DSGC forms an independent mosaic that tiles the retina with little dendritic overlap (Amthor and Oyster, 1995). Thus, in the rabbit that each point on the retina falls within the receptive fields of DSGCs sensitive to motion in each of four cardinal directions.

How does direction selectivity emerge during development? The generation of direction selective responses in the retina requires asymmetric wiring of inhibitory starburst amacrine

Correspondence to: Justin Elstrott.

*Chichilnisky and Feller contributed equally to the work

cells (SBACs) onto the On-Off DSGC dendritic arbor (Barlow and Levick, 1965; Fried et al., 2002; Yoshida et al., 2001); for reviews see (Demb, 2007; Taylor and Vaney, 2003; Vaney and Taylor, 2002). There are two primary models for how this asymmetric wiring might emerge. In the first model, patterned neural activity, such as correlated activity in the retina originating from either vision or spontaneous bursts known as retinal waves, provides an instructive cue for the establishment of direction selectivity. In the second model, direction selectivity is "hardwired", arising from molecular matching between subsets of processes of starburst amacrine cells and DSGCs.

Four recent lines of evidence suggest that patterned activity, rather than molecular cues, is required for the establishment of direction selectivity. First, the establishment of direction selectivity in primary visual cortex requires visual experience during a critical period of development immediately following eye-opening (Li et al., 2006). This distinguishes direction selectivity from other cortical maps such as ocular dominance and orientation tuning, which are both present at eye-opening and are relatively insensitive to dark rearing (White et al., 2001). Second, work on spike-timing dependent learning rules has indicated that direction selective responses can emerge spontaneously from training with directional moving stimuli (Mehta et al., 2002). Indeed, intensive training with directional stimuli artificially induces direction tuning in tectal neurons, which are not normally direction selective (Engert et al., 2002). Third, the development of sensory-motor reflexes generally requires sensory experience. In the optokinetic reflex, the gain of the visually driven eye movement must be tuned to minimize the extent of "retinal slip" in order to stabilize the visual scene. The optokinetic reflex is first observed in a mouse at postnatal day 21 (P21), approximately 8 days after eyes open (Faulstich et al., 2004), and is diminished after a period of dark rearing (McMullen et al., 2004). Fourth, no molecular-based mechanism has yet been identified that could mediate the asymmetric wiring pattern of inhibitory inputs onto an individual DSGC along one of four distinct cardinal axes. Though molecular gradients that uniquely determine location along the dorsal-ventral (D–V) and nasal-temporal (N–T) axes exist in the retina (Flanagan, 2006; McLaughlin and O'Leary, 2005), DSGCs at the same D–V, N–T location would need to respond differently to the gradients in order to wire the null side inhibition along all four cardinal axes.

The development of direction selectivity in the retina has not been fully explored. Older studies reported that retinal ganglion cells (RGCs) with asymmetric responses to moving stimuli were detected around the time of eye opening in rabbit (Bowe-Anders et al., 1975; Masland, 1977), and that the distribution of preferred directions was not biased by repeated presentations of moving gratings during development (Daw and Wyatt, 1974). Here we directly test the hypothesis that patterned activity induced by early visual responses is necessary for the establishment of On-Off DSGCs.

First, we characterize direction selective circuits in adult mice using novel multielectrode arrays that record simultaneously from hundreds of RGCs (Frechette et al., 2005; Litke A.M., 2004; Shlens et al., 2006). Isolated retinas were stimulated with drifting gratings and On-Off DSGCs were identified based on strict criteria (see Methods and Supplementary Figure 1). In agreement with previous studies (Weng et al., 2005), we found robust On-Off DSGCs in the adult mouse. An example of all the On-Off DSGCs recorded simultaneously from a single adult mouse retina (postnatal day 45: P45) is shown in Figure 1b. The polar plot in Figure 1a summarizes the raw spike trains recorded from a single cell in response a drifting grating stimulus that moved across the retina in 16 directions. For each cell, we computed the vector sum of the response, with the length of the vector representing the strength of tuning and the angle of the vector defining the preferred direction of motion (see Methods). Similar to what has been observed in the rabbit retina using in vivo single unit recordings (Oyster and Barlow,

1967), On-Off DSGCs in the mouse retina respond most strongly to motion along each of four roughly perpendicular cardinal directions (Figure 1b).

Next, we determined the earliest age at which On-Off DSGCs could be identified. The first light-evoked responses are detected in mouse retina at P10 (Demas et al., 2003; Tian and Copenhagen, 2003), which is two to three days before the eyes open. These early responses require strong light flashes and are much weaker compared to responses at older ages. The earliest age at which we could elicit robust RGC firing by both increasing and decreasing the illumination was P14 (Supplementary Figure 2). These On and Off responses were still not at the adult level, consistent with previous studies concluding that the anatomy and physiology of RGCs are not fully mature in mice until P28 (Tian and Copenhagen, 2001, 2003), similar to the retinal development in rabbit (Bowe-Anders et al., 1975; Masland, 1977), ferret (Wang et al., 2001), and cat (Rusoff and Dubin, 1977; Tootle, 1993). However, we found that at P14, which is one or two days after the eye-opening, On-Off DSGCs were already present in the retina.

To test the role of visual experience in establishing On-Off DSGCs, we repeated the recordings in P14 dark reared mice. Despite the weakness of the light responses prior to eye-opening, previous studies indicate that light coming through the closed eyelids may provide a relevant pattern of activity for the development of visual circuits. Indeed, visual deprivation by dark rearing during this period alters the refinement of circuits within the retina and in the dorsal LGN (Sernagor et al., 2001; Sernagor and Grzywacz, 1996; Tian and Copenhagen, 2003); (Grubb and Thompson, 2004). To test whether limited vision, either through closed eyelids or from the brief visual experience between yee-opening and the P14 experiments, was necessary to establish direction selectivity, we assayed direction-selective responses in mice that were dark reared from P7 to the time of the experiments. We detected a large number of DSGCs in P14 dark-reared mice (Figure 1c–d), indicating that direction selectivity is established early in development and independent of visual experience.

Robust direction selective responses were detected despite the observation that P14 DSGCs had significantly lower firing rates in their preferred directions compared to adult DSGCs ($p < 0.01$; Supplementary Figure 3). In contrast, there was no difference between the adult and P14 DSGCs in the null direction firing rates. We would therefore expect P14 DSGCs to have more uniform response curves and, consequently, broader tuning widths. To quantify the tuning width of each cell, we used a fit to its direction-selective response curve (see Methods; Figure 2a, insets). In the adult retina, tuning widths varied between 70–150 degrees, with the more broadly tuned cells exhibiting a more uniform distribution of firing rates across stimulus directions (Figure 2a). As expected, the tuning width distributions for both the P14 and P14 dark reared were shifted to broader values compared to the adult distribution (Figure 2b). Most importantly, though, both normal and dark reared P14 mice exhibited DSGCs with well-defined null directions.

In summary, the presence of directional tuning at P14 indicates that there is sufficient null side inhibition at the time of eye-opening for robust direction selectivity. The null side firing rate is dependent on the strength of the inhibitory inputs onto DSGCs, whereas firing rate for stimuli moving in the preferred direction is determined primarily by the strength of the excitatory inputs. Therefore the lower preferred direction firing rates at P14 compared to adult suggest that effective null side inhibition onto DSGCs is established before the maturation of the excitatory pathways and/or the spike generating mechanisms in DSGCs.

We have excluded the role of visual experience in the establishment of direction selectivity, and concluded that the null-side inhibition provided by SBACs onto DSGCs is wired very early in development. Could some form of patterned activity other than vision instruct this early

wiring? One strong candidate is retinal waves: spontaneous bursts of correlated activity that spread across the ganglion cell layer of the retina prior to eye-opening (for reviews see: Firth et al., 2005; Torborg and Feller, 2005; Wong, 1999). In particular, cholinergic retinal waves, which appear during the first postnatal week, are generated by the same starburst amacrine cells that underlie the null side inhibition in DSGCs (Zheng et al., 2006; Zheng et al., 2004). SBACs and DSGCs costratify early in development (Stacy and Wong, 2003), and show tightly correlated activity during this stage of retinal waves (Zheng et al., 2006; Zheng et al., 2004; Zhou, 1998). This evidence suggests that cholinergic retinal waves, which are directional in their propagation properties, could provide instructions for the asymmetric wiring between SBACs and DSGCs during the first week after birth (Demb, 2007; Weng et al., 2005).

To determine whether cholinergic retinal waves are necessary for establishing direction selectivity, we examined mice lacking the β2 subunit of the nicotinic acetylcholine receptor (β2 −/−). These mice lack normal propagating correlated activity during the first postnatal week (Bansal et al, 2003; McLaughlon et al., 2003, Cang et al, 2005), though there is evidence that β2 −/− mice exhibit non-cholinergic propagating activity under some conditions (Singer et al., 2001; Ballesteros, J. M., Sun, C., Goloshchapov, A. V., Cheng H. J. and Chalupa L. M, poster D23 SFN, 2007; David Feldheim personal communication). Even though significant local correlations persist in β2 −/− mice, these mice lack the propagating waves that correlate the firing of SBACs and DSGCs in a sequential manner (Torborg et al., 2004). Characterizing DSGCs in β2 −/− mice therefore allows us to directly test whether early retinal waves play an instructive role in the establishment of direction selectivity.

If patterned activity in the form of cholinergic waves were necessary for establishing DSGCs, we would expect direction selectivity in β2 −/− mice to be grossly disrupted. However, we found well-tuned DSGCs in β2 −/− mice at P14 (Figure 2c). This was despite the fact that the DSGCs in P14 β2 −/− mice were fewer in number compared to the P14 WT, consistent with the observation that signaling via nicotinic acetylcholine receptors (nAChRs) strongly modulates the amplitude of DSGC responses in adult mice (Weng et al., 2005) and rabbits (Kittila and Massey, 1997). Indeed, we found that acute blockade of β2-containing nAChRs with di-hydro-β-erthroidine (8μM) significantly reduced the firing rate of DSGCs in P14 WT mice (n=3 cells, data not shown). Despite the relative sparseness of detected DSGCs, β2 −/− mice showed narrow directional tuning that was not significantly different from adult WT mice (Figure 2b). The presence of strong direction selective responses with complete null-side inhibition in β2 −/− mice indicates that the asymmetric wiring underlying the generation of direction selectivity can occur independent of cholinergic retinal waves.

The finding that visual experience and cholinergic retinal waves are not necessary for the establishment of direction selectivity does not completely eliminate a role for neural activity in the process. First, there may be a role for glutamatergic retinal waves, which appear between P11 and P14 (Torborg and Feller, 2005). Glutamatergic retinal waves coexist with visual responses and are thought to be mediated by bipolar cells, whose inputs are symetrically distributed onto DSGCs (Jeon et al., 2002). Whether SBACs and DSGCs are correlated by glutamatergic waves, is not known. Second, spontaneous activity that locally correlates the firing between SBACs and DSGCs but does not propagate across the retina may still be critical for the establishment of the inhibitory synapses that shape the final light responses of DSGCs (Huang et al., 2007; Maffei et al., 2006; Tao and Poo, 2005).

Thus far we have shown that the establishment of direction selectivity does not require patterned activity in the form of early light responses or cholinergic retinal waves that correlate the firing of starburst amacrine cells and DSGCs. These findings indicate that molecular markers rather than correlated activity are likely to be critical for establishing DSGCs. We

would thus predict that the alignment of the DSGC preferred directions along the four cardinal axes would also be established independent of visual experience.

To assess the development of the cardinal axes, we first characterized the axes in adult mice. By pooling across preparations, we were able to count the fraction of total DSGCs belonging to a 90 degree bin centered at each cardinal direction. Though we were careful to align the retinas in a consistent manner on the array (see Methods), we deliberately chose a large bin size to account for the variability in placement of about ± 10 degrees. In the adult, the preferred directions of the DSGCs formed four clear clusters corresponding to the four cardinal directions (Figure 1b and 3a). Similar to previous studies of rabbit DSGCs (Oyster, 1968), the fraction of cells belonging to each cardinal direction was not uniformly distributed (Figure 3a; $p < 0.05$, χ^2 test of uniformity). However, the distributions along the temporal-nasal and ventral-dorsal axes were roughly symmetric, in that the cells that prefer two opposite directions of motion were roughly the same in number (ratio of temporal to nasal quadrant count: 1.107, $p = 0.3281$; ventral to dorsal: 1.583, $p = 0.0887$; see Methods).

The pooled P14 WT data also showed a non-uniform distribution of cells among the four cardinal directions (Figure 3b; $p < 0.001$, χ^2 test of uniformity). In addition, the representation of opposite directions along the same axis was strongly biased, with temporal and ventral quadrants being significantly overrepresented compared to their opposites (ratio of temporal to nasal quadrant count: 4.154, $p = 0.0001$; ventral to dorsal: 3.461, $p = 0.0001$). Figure 3c illustrates this asymmetry along both temporal-nasal and ventral-dorsal axes at P14 by showing the fractions of cells belonging to the two quadrants along each axis.

To further quantify the differences in the distribution of preferred directions of On-Off DSGCs at P14 and in the adult, we compared the relative abundance of cells on a quadrant-by-quadrant basis. We constructed 95% confidence intervals for each adult cardinal direction by resampling the adult data (see Methods), and found that the relative represenation of the nasal and ventral directions was significantly changed between P14 and adult (Figure 3d). To exclude the influence of a sampling bias, we verified that this effect was robust to variations of the cell selection criteria (see Methods).

What could explain the biases in the distributions of DSGC preferred directions seen at P14? Since RGC differentiation is largely completed by the time of eye opening (Sernagor et al., 2001), the On-Off DSGC mosaics corresponding to the four preferred directions are likely to be formed at P14. It is possible, however, that the four cell types are not equally responsive to light at this age. Indeed, the synaptic contacts between RGCs and bipolar cells only start to form around the time of eye opening (Sherry et al., 2003). It is therefore possible that the bipolar cell inputs onto the four On-Off DSGC mosaics mature in a stereotyped order during development, starting with the temporal and ventral directions of motion.

In summary, at the time of eye-opening we observed well-established DSGCs in the mouse retina, with nearly normal tuning and an organized but asymmetrical distribution of the preferred directions. These findings indicate that patterned activity containing directional information, either from visual experience or from cholinergic retinal waves which correlate the firing of starburt amacrine cells and DSGCs, is not necessary to establish the retinal circuits that mediate direction selectivity, though it may be involved in the refinement of these circuits. This is in sharp contrast to the primary visual cortex, where dark rearing during an early critical period prevented the establishment of direction selective cells (Li et al., 2006), and to On-Off segregation in the retina, where dark rearing disrupted the normal development of the dendritic stratification and the receptive fields of On and Off RGCs (Tian and Copenhagen, 2003). In addition, our data suggest that the excitatory drive, presumably from bipolar cell contacts, to the four subtypes of DSGCs emerges in a stereotyped order beginning with DSGCs preferring

temporal and ventral motion. Together, these results have implications for understanding how neural circuits are wired during development to perform behaviorally relevant computations, and they show that some components of sensory-motor reflexes are established independent of visual activity.

METHODS

Animals

Mice with heterozygous alleles of the β2 subunit of the nAChR (β2 +/−) were originally provided from Dr. Art Beaudet from Baylor College of Medecine (Xu et al., 1999). These mice were bred after backcrossing onto a C57BL/6 strain for many generations. The genotypes were determined according to the published protocol (Xu et al., 1999). C57BL/6 mice obtained from Harlan labs were used for all WT recordings. Dark reared litters (mothers and pups) were raised in darkness from P7 to P14 and monitored using infrared goggles. Mice not used for dark rearing experiments were maintained on a 12h light/dark cycle. Adult mice used in the recordings ranged in age from P28 to P45. All procedures were approved by the University of California, San Diego Institutional Animal Care and Use Committee and conformed to Salk Institute guidelines.

Acute Retina Preparation

All dissections were performed using dim red ambient light and infrared illumination on the dissection scope to prevent bleaching of the retinas. All mice were dark adapted for at least 60 minutes before the experiment. Animals were anesthetized with an IP injection of 100 mg/kg ketamine and 10 mg/kg xylazine prior to decapitation. After enucleation of the right eye, the eye was transferred to buffered Ames medium. Next, the eye was hemisected posterior to the ora serrata; and the cornea, lens, and vitreous were removed with forceps. We used blood vessel landmarks visible through the retina on the choroid to mark the ventral axis of the eyecup prior to removing the pigment epithelium with forceps. Next, we hemisected the isolated retina along the nasal-temporal axis as indicated by the landmarks. For all recordings, we used retina from the dorsal region of the right eye to minimize the variability across preparations. Stimulus motion was defined in the coordinates of an isolated retina, e.g. dorsal motion moved towards the dorsal part of the retina. These directions are flipped for the intact animal due to the optics of the lens.

Once a piece of dorsal retina had been isolated, it was placed ganglion-cell side down onto a custom-built multielectrode array. Three types of arrays were used: 61-electrode arrays with 5μm diameter electrodes and 60μm spacing, 61 electrode arrays with 5μm diameter electrodes and 30μm spacing, and 512 electrode arrays with 5μm diameter electrodes and 60μm spacing (Frechette et al., 2005; Litke A.M., 2004; Shlens et al., 2006). The piece of retina was aligned so that the nasal-temporal axis was parallel to the bottom of the array, with a variability of roughly ± 10 degrees. Once the piece had been aligned, a dialysis membrane was used to hold the retina in place on the array (Spectra/Por 6 RC dialysis tubing, MWCO 25,000). The array was superfused with Ames' solution (~ 220 ml/hr) bubbled with 95% O_2 and 5% CO_2 and maintained at 34–35° C, pH 7.4.

Light Stimulation

The photoreceptor layer of the isolated piece of retina was stimulated from above with an optically reduced image of a CRT monitor focused with a microscope objective, centered on the array, and refreshing at 120 Hz (gray screen intensity = 1623 491-nm equivalent photons/μm^2/sec). For most experiments, the retina was stimulated with 5 repetitions of full-field square wave gratings moving in one of 16 randomly interleaved directions with each presentation lasting 10 seconds followed by 3 seconds of gray screen (800 μm/period, 1.066 sec/period,

velocity = 25 degrees/sec for the adult mouse (Remtulla and Hallett, 1985)). In some 61-electrode recordings, full-field sinusoidal gratings were used (400 μm/period, 0.533 sec/period, velocity = 25 degrees/sec for the adult mouse).

Data Analysis

The voltage trace recorded on each electrode was sampled at 20 kHz and stored for offline analysis. Spikes that crossed threshold were sorted according to the principal components of their voltage waveforms on individual electrodes (for arrays with 60μm electrode spacing) or on a set of neighboring electrodes (for arrays with 30μm spacing). Spikes were first projected into the first 5 principal component dimensions where an expectation maximization algorithm was used to group spikes based on a mixture of Gaussians model (Litke A.M., 2004). All resulting spike clusters were inspected manually in the principal component space.

To verify that each cluster came from a single cell, the rate of refractory period violations was estimated using the number of interspike intervals between 0.5 and 1.2 msec. Only the clusters where refractory period violations represented less than 10% of all spikes were used for the subsequent analysis. In addition, cells with an average firing rate of less that 1Hz, and cells with unstable background firing (a larger than 75% decrease, as measured in a 260 sec window in the beginning and at the end of the recording) where excluded from consideration.

For a given cell, the response to motion in each of the 16 stimulus directions was measured as the mean firing rate during a 10 sec stimulus presentation, averaged across stimulus repetitions. The shape of the resulting tuning curve did not change when median inter-spike-intervals were used instead of the mean firing rates. The tuning curves were fit with the von Mises distribution (Oesch et al., 2005):

$$R=R_{\max}\, e^{k\cos(x-\mu)}/e^{k}, \tag{1}$$

where R is the response to motion in a given stimulus direction x in radians, R_{max} is the maximum response, μ is the preferred direction in radians (defined below), and k is the concentration parameter accounting for tuning width. The tuning width of each cell was estimated as the full width at half height (fwhh) of the von Mises fit using the following equation derived from (1):

$$fwhh=2\theta, \tag{2}$$

where

$$\theta=a\cos\left[\frac{\ln\left(\frac{1}{2}e^{k}+\frac{1}{2}e^{-k}\right)}{k}\right]. \tag{3}$$

The preferred direction of every cell was determined by a vector sum of the normalized responses to motion in all 16 stimulus directions. Before the summation, the response to motion in each direction on a given repetition was normalized by dividing by the total number of spikes elicited during that repetition across directions. Averaging the resulting vector sums across repetitions yielded the preferred direction vector. For a given cell, the magnitude of the response in the preferred direction could vary from 0 (no direction preference) to 1.

On-Off direction selective cells were isolated based on two criteria. First, the direction selective index was calculated for each cell:

$$D.I.=\frac{(pref-null)}{(pref+null)}$$

where *pref* is the average response in the preferred direction, defined as the stimulus direction closest to the vector sum, and *null* is the stimulus direction 180 degrees opposite *pref*. Cells

with a *D.I.* > 0.6 were classified as direction selective. Next, the On-Off sensitivity of these cells was quantified based on the power spectra of responses to drifting square wave or sinusoidal gratings (Supplementary Figure 1). Cells with a prominent f1 component (f2/f1 < 1) were classified as On DSGCs and excluded from the analysis.

To verify that the distribution of preferred directions among the On-Off DSGCs was not biased by cell selection, we varied independently each of the 5 selection parameters: the minimum average firing rate, maximum firing rate instability, maximum rate of refractory period violations, minimum value of the direction selectivity index, and the minimum f2/f1 ratio. Depending on the parameter, it could be varied between 25% and up to 300% of its original value without changing the relative fraction of On-Off DSGCs that fall into each of the four quadrants in Figure 3a & b.

To compute the 95% confidence intervals (shaded gray in Figure 3c) for the ratio of cells in opposing quadrants, sample distributions were created by drawing from either an adult or P14 distribution with replacement, and calculating the fraction of cells in each quadrant for each sample. This procedure was repeated 10,000 times, resulting in four non-Gaussian distributions of axis ratios (one for the adult temporal-nasal axis, another for adult ventral-dorsal axis, and same for P14). We identified the confidence intervals based on the upper and lower 2.5% boundaries of these distributions. A similar procedure was used to calculate the error bars in Figure 3d. Here the samples were drawn only from the adult distribution, resulting in Gaussian distributions of possible values for each cardinal direction, centered at the actual value. The standard deviations of these distributions were used as the error bars for each direction.

Supplementary Material

Refer to Web version on PubMed Central for supplementary material.

Acknowledgements

We thank J. Gauthier for working on the initial development of mouse multi-electrode array recordings. We thank W. Dabrowski, A. Grillo, M. Grivich, D. Gunning, S. Kachiguine, K. Mathieson, D. Petrusca, and J. Shlens for technical development. We thank G. Field for assistance with light intensity measurements, C. Hulse for technical assistance, and J. Bonaguro for figure suggestions. This work was supported by the McKnight Foundation (AML & EJC), NSF Grant PHY-0417175 (AML), NIH Grant EY018003 (EJC), NIH Grant R01EY13528 (MBF), a NSF Graduate Research Fellowship (JE), German Academic Exchange Service (DAAD) and German Research Foundation (DFG) (MG), and a Career Award at the Scientific Interface from the Burroughs Wellcome Fund (AS).

REFERENCES

Amthor FR, Oyster CW. Spatial organization of retinal information about the direction of image motion. Proc Natl Acad Sci U S A 1995;92:4002–4005. [PubMed: 7732021]

Bansal A, Singer JH, Hwang BJ, Xu W, Beaudet A, Feller MB. Mice lacking specific nicotinic acetylcholine receptor subunits exhibit dramatically altered spontaneous activity patterns and reveal a limited role for retinal waves in forming ON and OFF circuits in the inner retina. J Neurosci 2000;20:7672–7681. [PubMed: 11027228]

Barlow HB, Hill RM. Selective sensitivity to direction of movement in ganglion cells of the rabbit retina. Science 1963;139:412–414. [PubMed: 13966712]

Barlow HB, Levick WR. The mechanism of directionally selective units in rabbit's retina. J Physiol 1965;178:477–504. [PubMed: 5827909]

Bowe-Anders C, Miller RF, Dacheux R. Developmental characteristics of receptive organization in the isolated retina-eyecup of the rabbit. Brain Res 1975;87:61–65. [PubMed: 1120256]

Cang J, Reteria RC, Kaneko M, Liu X, Copenhagen DR, Stryker MP. Development of precise maps in visual cortex requires patterned spontaneous activity in the retina. Neuron 2005;48:797–809. [PubMed: 16337917]

Daw NW, Wyatt HJ. Raising rabbits in a moving visual environment: an attempt to modify directional sensitivity in the retina. J Physiol 1974;240:309–330. [PubMed: 4421344]

Demas J, Eglen SJ, Wong RO. Developmental loss of synchronous spontaneous activity in the mouse retina is independent of visual experience. J Neurosci 2003;23:2851–2860. [PubMed: 12684472]

Demb JB. Cellular mechanisms for direction selectivity in the retina. Neuron 2007;55:179–186. [PubMed: 17640521]

Engert F, Tao HW, Zhang LI, Poo MM. Moving visual stimuli rapidly induce direction sensitivity of developing tectal neurons. Nature 2002;419:470–475. [PubMed: 12368854]

Faulstich BM, Onori KA, du Lac S. Comparison of plasticity and development of mouse optokinetic and vestibulo-ocular reflexes suggests differential gain control mechanisms. Vision Res 2004;44:3419–3427. [PubMed: 15536010]

Firth SI, Wang CT, Feller MB. Retinal waves: mechanisms and function in visual system development. Cell Calcium 2005;37:425–432. [PubMed: 15820390]

Flanagan JG. Neural map specification by gradients. Curr Opin Neurobiol 2006;16:59–66. [PubMed: 16417998]

Frechette ES, Sher A, Grivich MI, Petrusca D, Litke AM, Chichilnisky EJ. Fidelity of the ensemble code for visual motion in primate retina. J Neurophysiol 2005;94:119–135. [PubMed: 15625091]

Fried SI, Munch TA, Werblin FS. Mechanisms and circuitry underlying directional selectivity in the retina. Nature 2002;420:411–414. [PubMed: 12459782]

Grubb MS, Thompson ID. The influence of early experience on the development of sensory systems. Curr Opin Neurobiol 2004;14:503–512. [PubMed: 15321072]

Huang ZJ, Di Cristo G, Ango F. Development of GABA innervation in the cerebral and cerebellar cortices. Nat Rev Neurosci 2007;8:673–686. [PubMed: 17704810]

Jeon CJ, Kong JH, Strettoi E, Rockhill R, Stasheff SF, Masland RH. Pattern of synaptic excitation and inhibition upon direction-selective retinal ganglion cells. J Comp Neurol 2002;449:195–205. [PubMed: 12115689]

Kittila CA, Massey SC. Pharmacology of directionally selective ganglion cells in the rabbit retina. J Neurophysiol 1997;77:675–689. [PubMed: 9065840]

Li Y, Fitzpatrick D, White LE. The development of direction selectivity in ferret visual cortex requires early visual experience. Nat Neurosci 2006;9:676–681. [PubMed: 16604068]

Litke AM, Bezayiff N, Chichilnisky EJ, Cunningham W, Dabrowski W, Grillo AA, Grivich M, Grybos P, Hottowy P, Kachiguine S, Kalmar RS, Mathieson K, Petrusca D, Rahman M, Sher A. What does the eye tell the brain? Development of a system for large-scale recording of retinal output activity. IEEE Transactions on Nuclear Science 2004;51:1434–1440.

Maffei A, Nataraj K, Nelson SB, Turrigiano GG. Potentiation of cortical inhibition by visual deprivation. Nature 2006;443:81–84. [PubMed: 16929304]

Masland RH. Maturation of function in the developing rabbit retina. J Comp Neurol 1977;175:275–286. [PubMed: 903424]

McLaughlin T, O'Leary DD. Molecular gradients and development of retinotopic maps. Annu Rev Neurosci 2005;28:327–355. [PubMed: 16022599]

McLaughlin T, Torborg CL, Feller MB, O'Leary DD. Retinotopic map refinement requires spontaneous retinal waves during a brief critical period of development. Neuron 2003;40:1147–1160. [PubMed: 14687549]

McMullen CA, Andrade FH, Stahl JS. Functional and genomic changes in the mouse ocular motor system in response to light deprivation from birth. J Neurosci 2004;24:161–169. [PubMed: 14715949]

Mehta MR, Lee AK, Wilson MA. Role of experience and oscillations in transforming a rate code into a temporal code. Nature 2002;417:741–746. [PubMed: 12066185]

Oesch N, Euler T, Taylor WR. Direction-selective dendritic action potentials in rabbit retina. Neuron 2005;47:739–750. [PubMed: 16129402]

Oyster CW. The analysis of image motion by the rabbit retina. J Physiol 1968;199:613–635. [PubMed: 5710424]

Oyster CW, Barlow HB. Direction-selective units in rabbit retina: distribution of preferred directions. Science 1967;155:841–842. [PubMed: 6019094]

Oyster CW, Takahashi E, Collewijn H. Direction-selective retinal ganglion cells and control of optokinetic nystagmus in the rabbit. Vision Res 1972;12:183–193. [PubMed: 5033683]

Remtulla S, Hallett PE. A schematic eye for the mouse, and comparisons with the rat. Vision Res 1985;25:21–31. [PubMed: 3984214]

Rusoff AC, Dubin MW. Development of receptive-field properties of retinal ganglion cells in kittens. J Neurophysiol 1977;40:1188–1198. [PubMed: 903800]

Sernagor E, Eglen SJ, Wong RO. Development of retinal ganglion cell structure and function. Prog Retin Eye Res 2001;20:139–174. [PubMed: 11173250]

Sernagor E, Grzywacz NM. Influence of spontaneous activity and visual experience on developing retinal receptive fields. Curr Biol 1996;6:1503–1508. [PubMed: 8939611]

Sherry DM, Wang MM, Bates J, Frishman LJ. Expression of vesicular glutamate transporter 1 in the mouse retina reveals temporal ordering in development of rod vs. cone and ON vs. OFF circuits. J Comp Neurol 2003;465:480–498. [PubMed: 12975811]

Shlens J, Field GD, Gauthier JL, Grivich MI, Petrusca D, Sher A, Litke AM, Chichilnisky EJ. The structure of multi-neuron firing patterns in primate retina. J Neurosci 2006;26:8254–8266. [PubMed: 16899720]

Simpson JI. The accessory optic system. Annu Rev Neurosci 1984;7:13–41. [PubMed: 6370078]

Singer JH, Mirtoznik RR, Feller MB. Potentiation of L-type calcium channels reveals nonsynaptic mechanisms that correlate spontaneous activity in the developing retina. J. Neurosci 2001;21:8514–8522. [PubMed: 11606640]

Stacy RC, Wong RO. Developmental relationship between cholinergic amacrine cell processes and ganglion cell dendrites of the mouse retina. J Comp Neurol 2003;456:154–166. [PubMed: 12509872]

Stahl JS. Using eye movements to assess brain function in mice. Vision Res 2004;44:3401–3410. [PubMed: 15536008]

Stewart DL, Chow KL, Masland RH. Receptive-field characteristics of lateral geniculate neurons in the rabbit. J Neurophysiol 1971;34:139–147. [PubMed: 5540575]

Tao HW, Poo MM. Activity-dependent matching of excitatory and inhibitory inputs during refinement of visual receptive fields. Neuron 2005;45:829–836. [PubMed: 15797545]

Taylor WR, Vaney DI. New directions in retinal research. Trends Neurosci 2003;26:379–385. [PubMed: 12850434]

Tian N, Copenhagen DR. Visual deprivation alters development of synaptic function in inner retina after eye opening. Neuron 2001;32:439–449. [PubMed: 11709155]

Tian N, Copenhagen DR. Visual stimulation is required for refinement of ON and OFF pathways in postnatal retina. Neuron 2003;39:85–96. [PubMed: 12848934]

Tootle JS. Early postnatal development of visual function in ganglion cells of the cat retina. J Neurophysiol 1993;69:1645–1660. [PubMed: 8509831]

Torborg C, Wang CT, Muir-Robinson G, Feller MB. L-type calcium channel agonist induces correlated depolarizations in mice lacking the beta2 subunit nAChRs. Vision Res 2004;44:3347–3355. [PubMed: 15536002]

Torborg CL, Feller MB. Spontaneous patterned retinal activity and the refinement of retinal projections. Prog Neurobiol 2005;76:213–235. [PubMed: 16280194]

Vaney DI, Taylor WR. Direction selectivity in the retina. Curr Opin neurobiol 2002;12:405–410. [PubMed: 12139988]

Vaney DI, Peichl L, Wassle H, Illing RB. Almost all ganglion cells in the rabbit retina project to the superior colliculus. Brain Res 1981;212:447–453. [PubMed: 7225878]

Wang GY, Liets LC, Chalupa LM. Unique functional properties of on and off pathways in the developing mammalian retina. J Neurosci 2001;21:4310–4317. [PubMed: 11404416]

Weng S, Sun W, He S. Identification of ON-OFF direction-selective ganglion cells in the mouse retina. J Physiol 2005;562:915–923. [PubMed: 15564281]

White LE, Coppola DM, Fitzpatrick D. The contribution of sensory experience to the maturation of orientation selectivity in ferret visual cortex. Nature 2001;411:1049–1052. [PubMed: 11429605]

Wong RO. Retinal waves and visual system development. Annu Rev Neurosci 1999;22:29–47. [PubMed: 10202531]

Xu W, Orr-Urtegar A, Nigro F, Gelber S, Sutcliffe CB, Armstrong D, Patrick JW, Role LW, Beaudet AL, De Biasi M. Multiorgan autonomic dysfunction in mice lacking the beta2 and beta4 subunits of neuronal nicotinic receptors. J. Neurosci 1999;19:9298–9305. [PubMed: 10531434]

Yoshida K, Watanabe D, Ishikane H, Tachibana M, Pastan I, Nakanishi S. A key role of starburst amacrine cells in originating retinal directional selectivity and optokinetic eye movement. Neuron 2001;30:771–780. [PubMed: 11430810]

Zheng J, Lee S, Zhou ZJ. A transient network of intrinsically bursting starburst cells underlies the generation of retinal waves. Nat Neurosci 2006;9:363–371. [PubMed: 16462736]

Zheng JJ, Lee S, Zhou ZJ. A developmental switch in the excitability and function of the starburst network in the mammalian retina. Neuron 2004;44:851–864. [PubMed: 15572115]

Zhou ZJ. Direct participation of starburst amacrine cells in spontaneous rhythmic activities in the developing mammalian retina. J Neurosci 1998;18:4155–4165. [PubMed: 9592095]

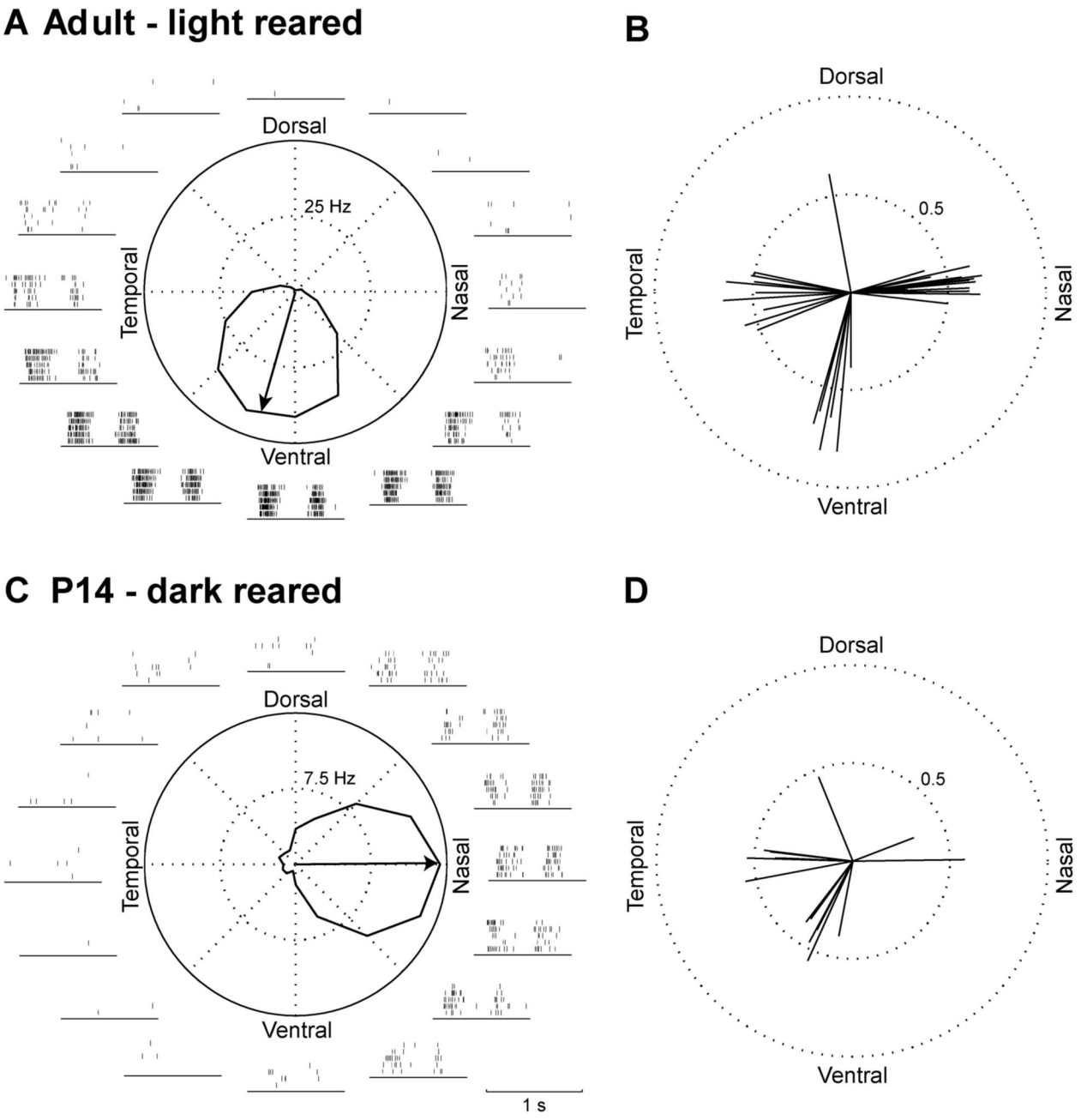

Figure 1. Responses of On-Off DSGCs to moving gratings reveal strong direction selectivity in the adult and P14 dark reared mouse

a & c. Polar-plot of mean spike rate response to motion in 16 directions across five repetitions. Spike traces for all directions are shown for one period of the moving grating. The tuning curve was obtained using the mean firing rate in response to each direction (see Methods). The arrow indicates mean preferred direction of the example cell. Adult: n = 31 cells; P14 dark reared: n = 15 cells. **b & d.** The preferred directions of all On-Off DSGCs within one adult preparation **(b)** fall clearly into four groups along the cardinal directions. The cardinal directions were more variable at P14 (see also Figure 3). The preferred direction of each cell is shown as the

normalized vector sum of the response, so that the length of each line indicates the normalized response magnitude.

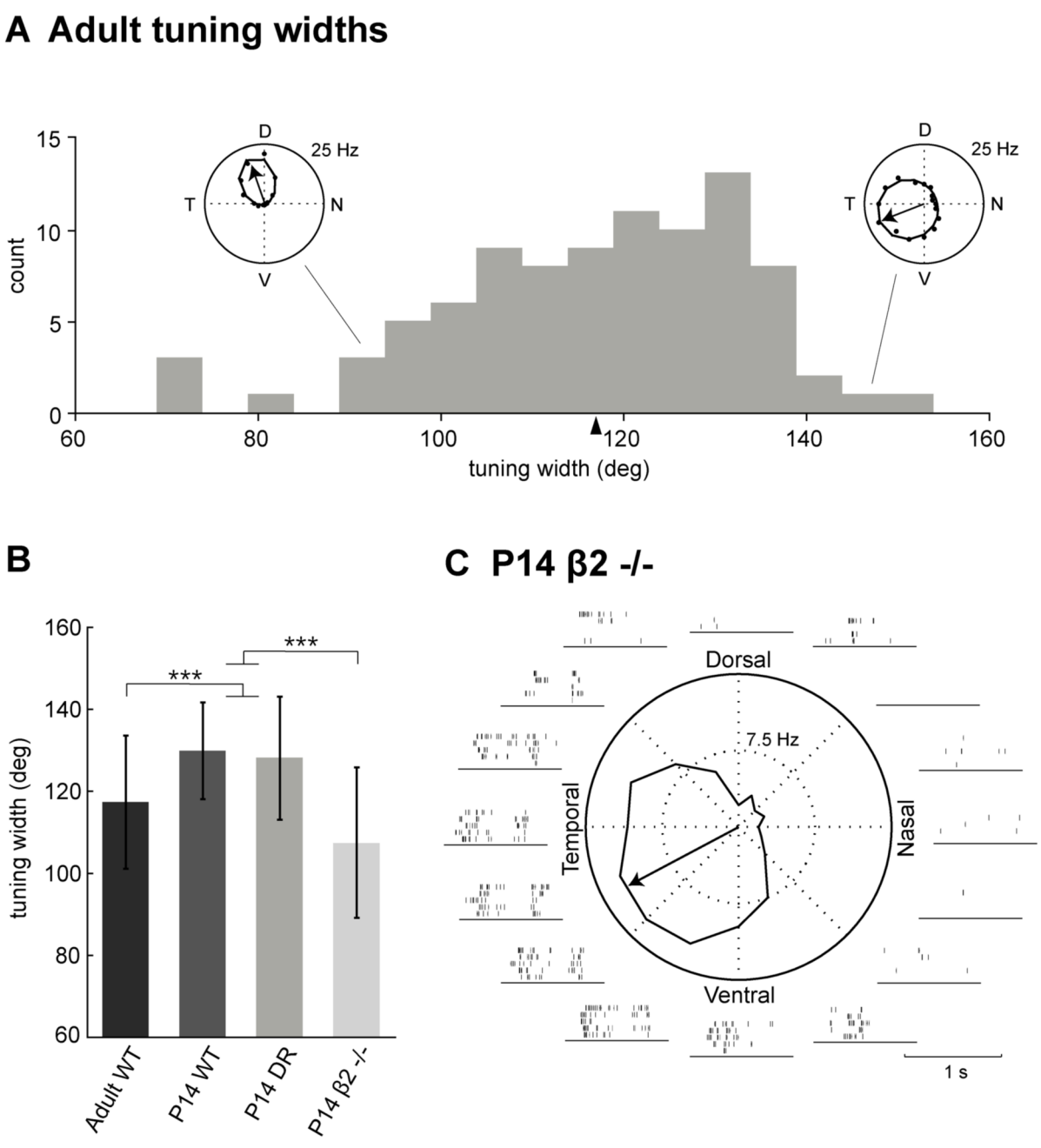

Figure 2. Population tuning widths change during development

a. Histogram shows the distribution of tuning widths (full width at half height of a von-Mises fit, see methods) of all adult WT cells (90 cells from 11 mice). Arrowhead shows mean value. Insets show the average responses (dots) and the von-Mises fits (lines) for two cells. The arrow indicates the preferred direction for each cell. **b.** A comparison of tuning widths across groups (adult n's same as above, P14 WT: n = 75 cells from 11 mice; P14 dark reared: n = 50 cells from 4 mice; P14 β2 −/−: n = 13 cells from 4 mice). The adult WT and P14 β2 −/− mice showed significantly narrower tuning than both the P14 WT and P14 dark reared mice ($p < .0001$; one-way ANOVA with Tukey post-hoc test). Data are presented as mean ± s.d. **c.** An example On-Off DSGC from a P14 β2 −/− mouse.

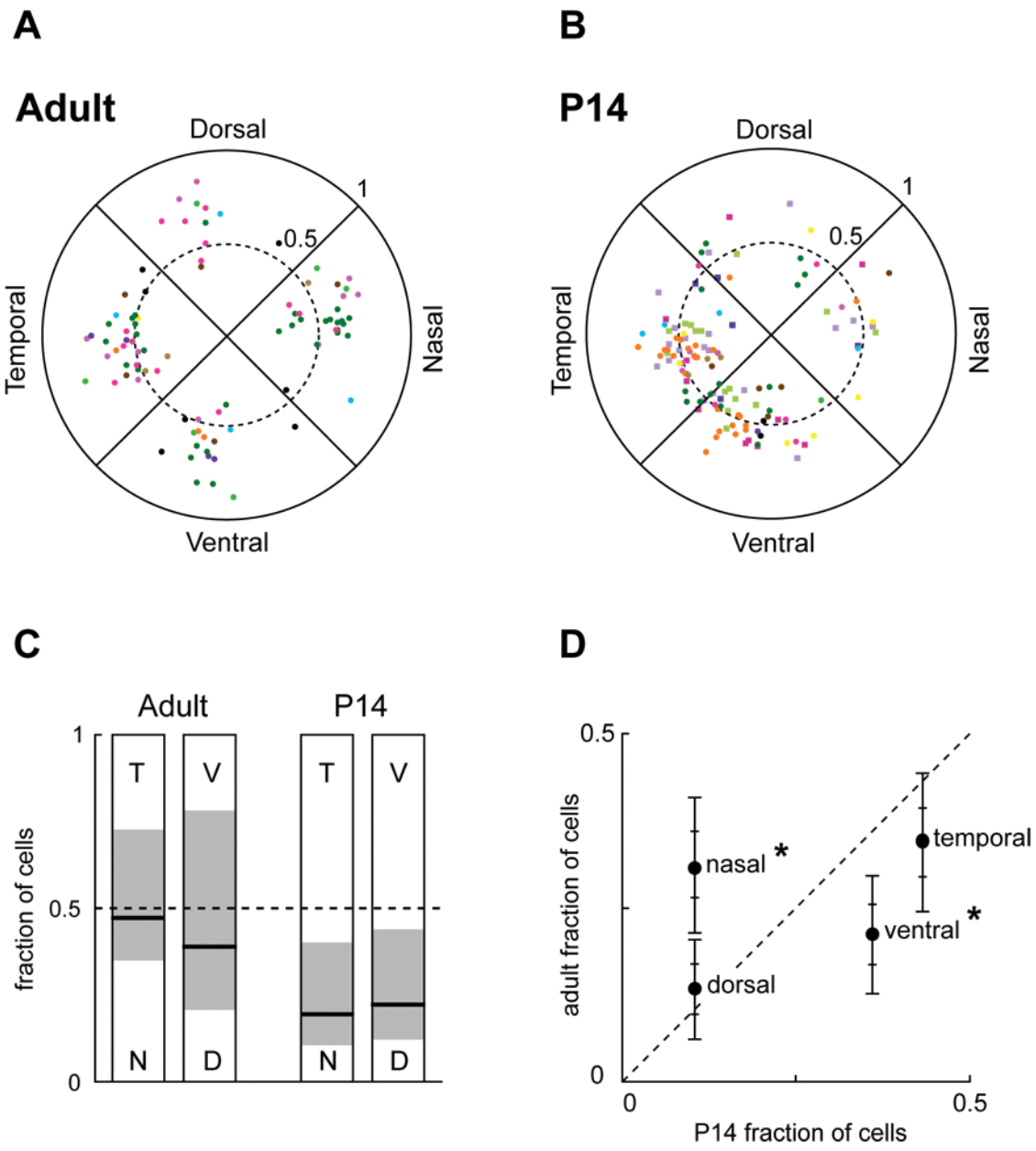

Figure 3. Distributions of preferred directions for On-Off DSGCs in adult and P14 mice

a & b. Scatter plot shows the preferred directions and normalized magnitudes of the responses of adult and P14 cells pooled across experiments (adult: n = 90 cells from 11 mice; P14: n = 125 cells from 15 mice). Each color represents data from a single experiment. At P14, squares are dark-reared mice; circles are normal mice. **c & d.** The fraction of cells belonging to each cardinal direction was calculated by grouping the data shown in **a & b** into 90 degree bins. **c.** The symmetry of preferred directions along a given axis (temporal-nasal or ventral-dorsal) was tested by calculating the fraction of cells falling in one quadrant along the axis (e.g. temporal) versus the fraction of cells in the opposite quadrant (e.g. nasal). A perfectly symmetric axis would have 50% of cells in opposite quadrants. The thick black bars shows the actual distribution of cells along the axes for adult and P14. The shaded gray regions show the 95% confidence interval around each value based on resampling of the adult and P14

distributions (see Methods). **d.** A comparison of adult and P14 distribution of preferred directions on a quadrant-by-quadrant basis. In case of a uniform distribution, each quadrant would encompass 25% of cells. The error bars show ±1 s.d (inner ticks) and ± 2 s.d. (outer ticks) based on resampling the adult distribution (see Methods). Directions whose error bars lie beyond the dashed line have P14 values significantly different from adult values.